Original Article

IJMEE

International Journal of Mechanical Engineering Education
2015, Vol. 43(4) 209–232

DOI: 10.1177/0306419015603893
ijj.sagepub.com
SAGE

Effects of a frictionless hinge on internal forces, deflections, and load capacity of beam structures

Vlado A Lubarda

Abstract

The redistribution of internal forces and deflections in a uniformly loaded propped cantilever and a fixed-end beam caused by the insertion of a frictionless hinge is evaluated for an arbitrary position of the hinge. This is accomplished by an extended use of the method of discontinuity functions to incorporate the slope discontinuity at the hinge, without the separation of structures into their constituting parts, as commonly done in other methods of analysis. It is shown that the insertion of a hinge in the middle of a propped cantilever increases the reactive moment at the fixed end two times. A hinge in the middle of a fixed-end beam increases its reactive moments by 50%, while the maximum deflection increases three times. The maximum allowable load is determined for all considered structures by using the classical and the limit design criteria. If a hinge is placed in a propped cantilever at the distance from its fixed end smaller than one-fourth of its span, the classical design criterion predicts that a hinged propped cantilever can transmit a greater distributed load than a propped cantilever without a hinge. However, according to the limit design criterion, the insertion of a hinge in a propped cantilever decreases the ultimate load for any location of a hinge. The insertion of a hinge in a fixed-end beam decreases the maximum load according to both, the classical and the limit design criteria. For the rectangular cross section, the ratio of the maximum loads according to the limit and the classical design criterion is constant and equal to 3/2 in the case of a hinge-relaxed propped cantilever, while it varies with the position of the hinge in the case of a hinge-relaxed fixed-end beam. The presented analysis and the obtained results are of interest for undergraduate engineering education in the courses of mechanics of materials and structural design.

Department of NanoEngineering and Mechanical and Aerospace Engineering, University of California, San Diego, USA

Corresponding author:
Vlado A Lubarda, Department of NanoEngineering, University of California, San Diego, 9500 Gilman Drive, La Jolla, CA 92093-0448, USA.
Email: vlubarda@ucsd.edu

Keywords
Allowable load, collapse mechanism, design criterion, discontinuity functions, hinge, limit analysis, ultimate load, yield stress

Introduction

The determination of deflected shape of elastic beam structures and their allowable loads according to the classical or the limit design criterion are classic problems of solid mechanics and engineering design (Beer et al., 2014; Budynas and Nisbett, 2014; Craig, 2011; Gere and Goodno, 2013). Nevertheless, an analytical examination of the effect of the location of an inserted frictionless hinge on the redistribution of internal forces and deflections, and the resulting changes of the load capacity of beam structures, have not been fully addressed or reported in the literature. Toward that goal, in this paper we consider two important structural beam problems, a propped cantilever and a fixed-end beam, with and without an inserted hinge, under a uniformly distributed load. Their elastic deflections and internal forces are determined by making an extended use of the method of discontinuity functions to incorporate the slope discontinuity at the hinge, without the separation of structures into their constituting parts, common to other types of analyzes. The utilized method significantly facilitates the analysis, but surprisingly has not yet been incorporated in the mechanics of materials textbooks, although it has been promoted in the journal literature fifty years ago (Brungraber, 1965). It is shown, inter alia, that the insertion of a hinge in the middle of a propped cantilever increases the reactive moment at the fixed end two times, while a hinge in the middle of a fixed-end beam increases its reactive moments by 50%. The mid-deflection of a fixed-end beam is increased three times by the introduction of a hinge in its mid-section. The maximum allowable load is determined by using the classical and the limit design criteria. According to the classical design criterion, if a hinge is placed in a propped cantilever at the distance from its fixed end smaller than one-fourth of its span ($a < L/4$), the hinged structure can, surprisingly, transmit a greater distributed load than a propped cantilever without a hinge. The maximum load that a hinged structure can transmit is about 46% greater than the maximum load transmitted by a propped cantilever without a hinge. However, according to the limit design criterion, the insertion of a hinge in a propped cantilever decreases the limit load for any a/L. On the other hand, the insertion of a hinge in a fixed-end beam decreases the maximum load according to both design criteria, for any position of a hinge. The classical design criterion in this case predicts the greatest load decrease if a hinge is placed at $a = 0.4171\ L$, the maximum load is about 61% of the maximum load transmitted by a fixed-end beam without a hinge. According to the limit design criterion, the load decrease is greatest for $a = 0.5\ L$, when it is 50% of the maximum load transmitted by a fixed-end beam without a hinge. For rectangular cross-sections, the ratio of the maximum load according to the limit and the classical design criteria is constant and equal to 3/2 in the case of a hinge-relaxed propped cantilever, while it varies with a/L in the case of a hinge-relaxed fixed-end beam.

Analysis of two beams connected by a hinge

A frictionless hinge connecting two beams cannot transmit a bending moment and thus does not place any restriction on the relative rotation of adjacent beams. The determination of deflections in a structure consisting of two beams connected by a hinge, such as one shown in Figure 1(a), by the integration of the corresponding differential equation requires a lengthy integration for each beam separately, unless discontinuity functions are used. The use of discontinuity functions for hinge-connected beam structures was first advocated by Brungraber (1965) and subsequently expanded upon by Failla (2011), Falsone (2002), and Yavari et al. (2000), but, surprisingly, the method has not yet found its place in solid mechanics textbooks, which include the use of discontinuity functions for the unhinged structures only. To demonstrate its effectiveness, the method is applied in this section to determine deflections and internal forces in a hinge-connected beam structure from Figure 1(a). The derived general results are then specialized to generate the solutions to two hinge-relaxed structures shown in Figure 1(b) and 1(c).

The Macaulay functions of integer degree $n \geq 0$ are defined by

$$\langle z-a\rangle^n = \begin{cases} 0, & z<a \\ (z-a)^n, & z \geq a \end{cases} \tag{1}$$

where the angle brackets $\langle\rangle$ are the so-called Macaulay brackets (e.g. Craig, 2011). The Macaulay functions can be conveniently used to represent a suddenly

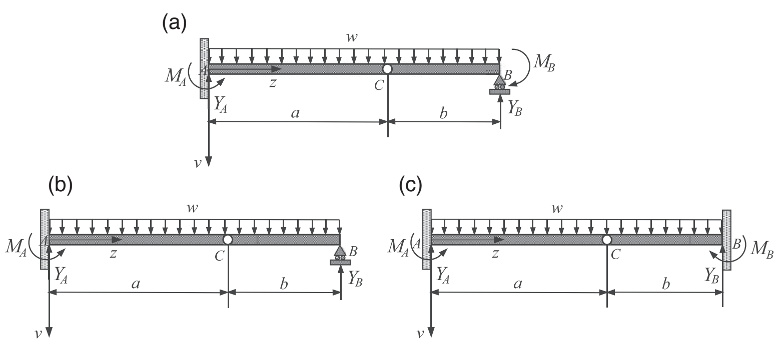

Figure 1. (a) Two beams connected by a hinge at C. The end A is fixed, and the end B is simply supported. The loading consists of a uniform load w applied along the entire length of the structure, and a concentrated moment M_B at the end B. The deflection of the beam is $v = v(z)$, where z is measured from A. (b) Two beams connected by a hinge at C. The end A is fixed, and the end B is simply supported. (c) Two cantilever beams connected by a hinge at C.

terminating or abruptly changing distributed load. A concentrated force is represented by a singularity function $\langle\rangle^{-1}$, which is singular at $z = a$ and zero for $z \neq a$ (unit impulse function). Similarly, a concentrated couple can be represented by a singularity function $\langle\rangle^{-2}$ (unit doublet function). The latter are defined so that the integrals of discontinuity functions are

$$\int \langle z-a\rangle^{n}\,\mathrm{d}z = \begin{cases} \langle z-a\rangle^{n+1}, & n \leq 0 \\ \dfrac{1}{n+1}\,\langle z-a\rangle^{n+1}, & n > 0 \end{cases} \tag{2}$$

Since the discontinuity of the shear force, i.e. the discontinuity of the third derivative of deflection, is represented by using the singularity function $\langle z-a\rangle^{-1}$, and the discontinuity of the moment (or second derivative of deflection) by using the singularity function $\langle z-a\rangle^{-2}$, the discontinuity of the first derivative of deflection (slope discontinuity) at the hinge can be incorporated in the analysis by using the singularity function $\langle z-a\rangle^{-3}$ (Brungraber, 1965).

With the so-introduced discontinuity functions, the governing differential equation for the deflection of the beam in Figure 1(a) can be written as

$$\begin{aligned} EIv''''(z) = {} & M_A\langle z\rangle^{-2} - Y_A\langle z\rangle^{-1} + EI\Delta v'_C\langle z-a\rangle^{-3} \\ & - Y_B\langle z-L\rangle^{-1} - M_B\langle z-L\rangle^{-2} + w\langle z\rangle^{0} \end{aligned} \tag{3}$$

The slope discontinuity at the hinge is denoted by $\Delta v'_C = v'(a^+) - v'(a^-)$. Respecting the rules of integration, equation (2), four consecutive integrals of equation (3) are

$$EIv'''(z) = M_A\langle z\rangle^{-1} - Y_A\langle z\rangle^{0} + EI\Delta v'_C\langle z-a\rangle^{-2} - Y_B\langle z-L\rangle^{0} - M_B\langle z-L\rangle^{-1} + w\langle z\rangle^{1} \tag{4}$$

$$EIv''(z) = M_A\langle z\rangle^{0} - Y_A\langle z\rangle^{1} + EI\Delta v'_C\langle z-a\rangle^{-1} - Y_B\langle z-L\rangle^{1} - M_B\langle z-L\rangle^{0} + \frac{1}{2}\,w\langle z\rangle^{2} \tag{5}$$

$$\begin{aligned} EIv'(z) = {} & M_A\langle z\rangle^{1} - \frac{1}{2}\,Y_A\langle z\rangle^{2} + EI\Delta v'_C\langle z-a\rangle^{0} - \frac{1}{2}\,Y_B\langle z-L\rangle^{2} - M_B\langle z-L\rangle^{1} \\ & + \frac{1}{6}\,w\langle z\rangle^{3} + EIv'(0)\langle z\rangle^{0}, \quad v'(0) = 0 \end{aligned} \tag{6}$$

$$\begin{aligned} EIv(z) = {} & \frac{1}{2}\,M_A\langle z\rangle^{2} - \frac{1}{6}\,Y_A\langle z\rangle^{3} + EI\Delta v'_C\langle z-a\rangle^{1} - \frac{1}{6}\,Y_B\langle z-L\rangle^{3} - \frac{1}{2}\,M_B\langle z-L\rangle^{2} \\ & + \frac{1}{24}\,w\langle z\rangle^{4} + EIv(0)\langle z\rangle^{0}, \quad v(0) = 0 \end{aligned} \tag{7}$$

The moment conditions at C and B are $v''(a) = 0$ and $EIv''(L) = M_B$ (with the assumed direction of M_B as shown in Figure 1(a)). In view of equation (5), they give

$$M_A - Y_A a = -\frac{1}{2}\, wa^2, \quad M_A - Y_A L = M_B - \frac{1}{2}\, wL^2 \tag{8}$$

which can be solved for Y_A and M_A to obtain

$$Y_A = \frac{1}{2}\, w(a+L) - \frac{M_B}{b}, \quad M_A = \frac{1}{2}\, waL - \frac{a}{b}\, M_B \tag{9}$$

The reaction Y_B follows from the closure condition $V(L^+) = -EIv'''(L^+) = 0$, from which $Y_B = wL - Y_A$, i.e.

$$Y_B = \frac{1}{2}\, wb + \frac{M_B}{b} \tag{10}$$

The boundary condition $v(L) = 0$ of zero deflection at the support B requires, from equation (7), that

$$\frac{1}{2}\, M_A L^2 - \frac{1}{6}\, Y_A L^3 + EI\Delta v'_C b = -\frac{1}{24}\, wL^4 \tag{11}$$

In view of equation (9), this yields an expression for the slope discontinuity at the hinge

$$EI\Delta v'_C = \frac{wL^3}{24}\left(1 - 3\,\frac{a}{b}\right) + \frac{M_B L^2}{6b}\left(2\,\frac{a}{b} - 1\right) \tag{12}$$

The internal force at the hinge is obtained from $Y_C = -EIv'''(a)$, which gives

$$Y_C = \frac{1}{2}\, wb - \frac{M_B}{b} \tag{13}$$

The expression for the slope at the support B is

$$EIv'(L) = -\frac{wa^4}{24}\left[\left(\frac{b}{a}\right)^4 + 4\,\frac{b}{a} + 3\right] + \frac{M_B b}{3}\left[1 + \left(\frac{a}{b}\right)^3\right] \tag{14}$$

The expression for the deflected shape is obtained by substituting equations (9) and (12) into equation (7). The presented derivation demonstrates the effectiveness of the method, which does not require the separation of the structure into two parts and the explicit imposition of the continuity conditions at the hinge, inherent to other methods of solution.

Analysis of a hinge-relaxed propped cantilever

If the moment at the support B vanishes ($M_B = 0$), the hinged structure from Figure 1(b) is obtained. The corresponding reactions and the slope discontinuity are, from equations (9) to (12)

$$Y_A = \frac{1}{2}\,w(a+L), \quad Y_B = Y_C = \frac{1}{2}\,wb, \quad M_A = \frac{1}{2}\,waL, \quad \Delta v'_C = \frac{wL^3}{24EI}\left(1 - 3\,\frac{a}{b}\right) \tag{15}$$

The overall deflected shape is

$$v(z) = \frac{wL^4}{24EI}\left[6\,\frac{a}{L}\left(\frac{z}{L}\right)^2 - 2\left(1+\frac{a}{L}\right)\left(\frac{z}{L}\right)^3 + \left(\frac{z}{L}\right)^4 + \frac{a}{L}\left(1 - 3\,\frac{a}{b}\right)\left\langle\frac{z}{a} - 1\right\rangle\right] \tag{16}$$

In particular, the deflection at the hinge is

$$v(a) = \frac{wa^3}{24EI}\,(3a + 4b) \tag{17}$$

Figures 2(a) and 2(b) show deflected shapes when the hinge is located at $a = 0.5L$ and $a = 0.3L$. In the former case the deflection is maximum at the hinge and equal to $v_C \simeq 18.23\ v_0$, where $v_0 = 10^{-3} wL^4/EI$. In the later case the deflection at the hinge is $v_C \simeq 4.16\ v_0$, while the maximum deflection is $v_{\max} \simeq 5.5\ v_0$, reached at $z \simeq 0.55L$, which is about 32% greater than v_C. If $a \simeq 0.3591\ L$, the slope $v'(a^+) = 0$ (Figure 2(c)). There is no slope discontinuity at C (passive hinge, $\Delta v'_C = 0$) if $b = 3a$, i.e. $a = L/4$ (Figure 2(d)). In this case the deflection at C is $v_C \simeq 2.44\ v_0$. The numerical evaluation of the maximum deflection was performed by executing the Matlab function [ζ,*fval*] = *fminbnd(fun,0,1)*, which returns a local minimizer ζ ($= z/L$) at which the function specified in the function_handle *fun* reaches its minimum value (*fval*) within the interval $0 < \zeta < 1$. The *fun* = $-\,v(z)$ is specified by equation (16). The Matlab details of this minimization procedure are included for educational purposes, because this simple exercise offers an opportunity for students to demonstrate their ability to use modern tools in engineering education, such as the Matlab software, which contributes to the fulfillment of the ABET student outcome criterion 3k (ABET, 2015).

Other aspects of the analysis can be pursued. For example, since the end slope of a simply supported beam is $wb^3/24EI$, the maximum deflection will occur to the right of the hinge if

$$\frac{wb^3}{24EI} > \frac{v(a)}{b}, \quad \text{i.e.,} \quad \left(\frac{b}{a}\right)^4 - 4\,\frac{b}{a} - 3 > 0 \tag{18}$$

By using the Matlab function *roots*(p) (Attaway, 2013) to find the roots of the polynomial whose coefficients are $p = [1, 0, 0, -4, -3]$, it follows that the inequality (18) holds provided that $b > 1.7844a$, i.e. $a < 0.3591L$.

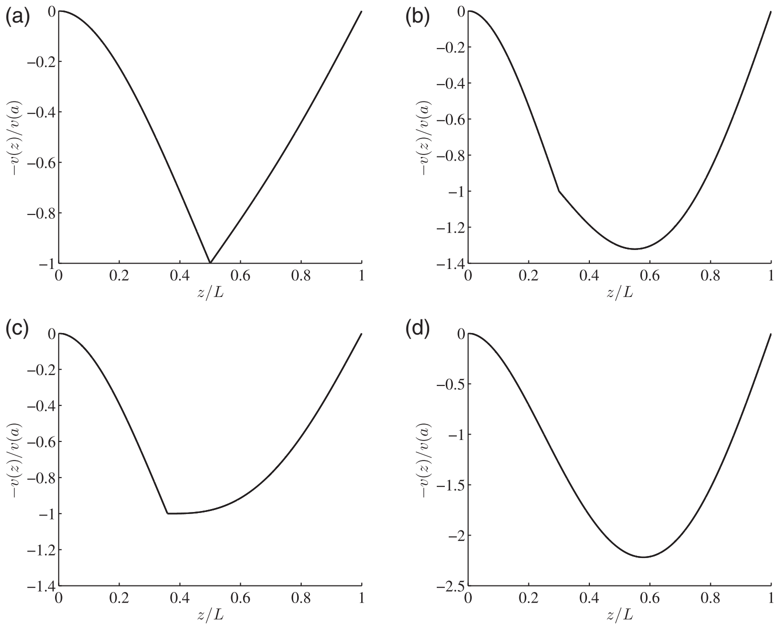

Figure 2. Deflected shapes of a hinge-connected beam structure from Figure 1(b) in the case when the hinge is placed at: (a) $a = 0.5L$; (b) $a = 0.3L$; (c) $a = 0.3591L$; and (d) $a = 0.25L$. The scaling factor for deflections is the magnitude of the deflection at the hinge, which is $v(a) \simeq 18.23\ v_0$ in case (a), $v(a) \simeq 4.16\ v_0$ in case (b), $v(a) \simeq 7.02\ v_0$ in case (c), and $v(a) \simeq 2.44\ v_0$ in case (d), where $v_0 = 10^{-3}\ wL^4/EI$. In case (c) the slope $v'(a^+) = 0$, and in case (d) the hinge is passive in the sense that $v'(a^-) = v'(a^+)$.

Analysis of hinge-connected cantilever beams

The reactions and deflected shape of a hinged structure made of two cantilever beams, shown in Figure 1(c), can be directly obtained from the derived general results by imposing the condition $v'(L) = 0$. From equation (14) it follows that the corresponding reactive moment is

$$M_B = \frac{wb}{8}\left(b + \frac{3a^3}{d^2}\right), \quad d^2 = a^2 + b^2 - ab \tag{19}$$

The other reactions follow from equations (9) and (10) as

$$Y_A = \frac{w}{8}\left(5a + \frac{3b^3}{d^2}\right), \quad Y_B = \frac{w}{8}\left(5b + \frac{3a^3}{d^2}\right), \quad M_A = \frac{wa}{8}\left(a + \frac{3b^3}{d^2}\right) \tag{20}$$

The symmetry of the expressions for Y_A and Y_B, and M_A and M_B, regarding the interchange of a and b, is noted in equations (19) and (20). The internal force at the hinge C is

$$Y_C = \frac{3w}{8}\frac{b^3 - ad^2}{d^2} = \frac{3w}{8}\frac{b^4 - a^4}{a^3 + b^3} \tag{21}$$

In the last step, the identity $a^3 + b^3 = (a+b)d^2$ was used. The slope discontinuity at the hinge C is

$$\Delta v'_C = \frac{wL^3}{48EI}\left(1 - 3\,\frac{ab}{d^2}\right) \tag{22}$$

The deflected shape of the beam follows from equation (7), and is given by

$$EIv(z) = \frac{1}{2}\,M_A z^2 - \frac{1}{6}\,Y_A z^3 + \frac{1}{24}\,wz^4 + EI\Delta v'_C\langle z - a\rangle \tag{23}$$

where Y_A, M_A, and $\Delta v'_C$ are specified by equations (20) and (22). In particular, the deflection of the hinge is

$$v(a) = \frac{wa^3b^3}{8EId^2} \tag{24}$$

There is no slope discontinuity at the hinge if $\Delta v'_C = 0$ in equation (22), i.e. if

$$\left(\frac{b}{a}\right)^2 - 4\,\frac{b}{a} + 1 = 0 \tag{25}$$

The solutions of this quadratic equation are $b/a = 2 \pm \sqrt{3}$. In terms of the ratio a/L, the two corresponding locations of the hinge are specified by $a = (1 \mp \sqrt{3}/3)L/2$ (i.e. $a \simeq 0.2113L$ and $a \simeq 0.7887L$), symmetrically positioned with respect to $a = 0.5L$ (Figure 3(a)). The deflection at C in either case is $v_C \simeq 1.158\ v_0$. The deflected shape in case $a = 0.5L$ is shown in Figure 3(b). Figures 3(c) and (d) show deflected shapes in cases $a = 0.25L$ and $a = 0.3L$. In the former case the deflection at the hinge is $v_C \simeq 1.883\ v_0$, while the maximum deflection is $v_{\max} \simeq 2.612\ v_0$ (reached at $z \simeq 0.479L$, and about 39% greater than v_C). In the latter case, $v'(a^+) \simeq 0$.

An important design question is to determine for which ratio a/L the maximum deflection in the structure does not occur at the hinge. The outcome of the analysis is that for $0 < a < 0.3043L$ the maximum deflection occurs to the right of C, and for

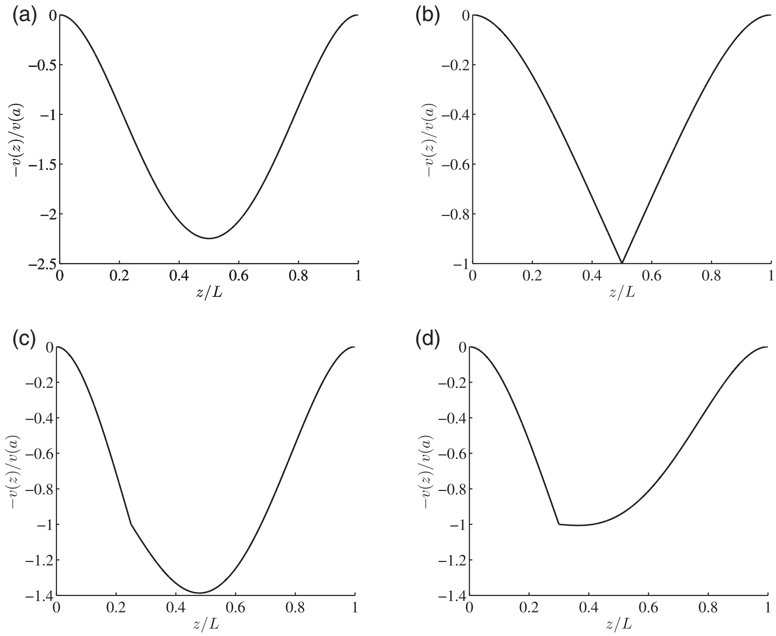

Figure 3. Deflected shapes of the beam structure from Figure 1(c) in the case when the hinge is placed at: (a) $a = 0.2113L$; (b) $a = 0.5L$; (c) $a = 0.25L$; and (d) $a = 0.3L$. The scaling factor for deflections is the magnitude of deflection at the hinge, which is $v(a) \simeq 1.158\ v_0$ in case (a), $v(a) \simeq 7.813\ v_0$ in case (b), $v(a) \simeq 1.883\ v_0$ in case (c), and $v(a) = 3.129\ v_0$ in case (d), where $v_0 = 10^{-3}\ wL^4/EI$.

$0.6957 < a < L$ to the left of C. In each case the location of the maximum deflection is specified by

$$z = \frac{1}{2w}\left[3Y_A - \left(9Y_A^2 - 24wM_A\right)^{1/2}\right], \quad 9Y_A^2 \geq 24wM_A \tag{26}$$

Redistribution of reactions in a propped cantilever by a hinge

It is important for the design purposes to evaluate the redistribution of reactions at A and B in a propped cantilever from Figure 4(a) (case I) caused by the insertion of a hinge (Figure 4(b), case II). The reactions in a propped cantilever of length L (e.g. Gere and Goodno, 2013) are

$$Y_A^I = \frac{5}{8}\,wL, \quad Y_B^I = \frac{3}{8}\,wL, \quad M_A^I = \frac{1}{8}\,wL^2 \tag{27}$$

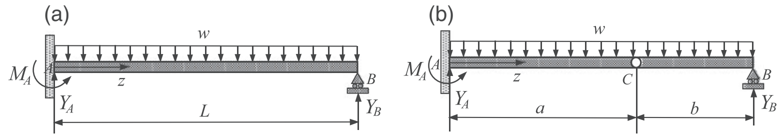

Figure 4. (a) A propped cantilever of length $L = a + b$ under uniform load w (case I). (b) A propped cantilever from part (a) with an inserted hinge at $z = a$ (case II).

The corresponding deflected shape is

$$v^I(z) = \frac{wL^4}{48EI}\left(\frac{z}{L}\right)^2\left[2\left(\frac{z}{L}\right)^2 - 5\,\frac{z}{L} + 3\right] \tag{28}$$

On the other hand, from equation (15), the reactions in a propped cantilever with a hinge at C (Figure 4(b)) are

$$Y_A^{II} = \frac{1}{2}\,w(2a+b), \quad Y_B^{II} = \frac{1}{2}\,wb, \quad M_A^{II} = \frac{1}{2}\,wa(a+b)$$

Thus, the redistribution of the reactions at A and B are specified by the following ratios

$$\frac{Y_A^{II}}{Y_A^I} = \frac{4(2a+b)}{5(a+b)}, \quad \frac{Y_B^{II}}{Y_B^I} = \frac{4b}{3(a+b)}, \quad \frac{M_A^{II}}{M_A^I} = \frac{4a}{a+b}$$

For example, a hinge in a propped cantilever of length L placed in the middle of its span $(a = b = L/2)$ increases the reactive moment at the fixed end two times $(M_A^{II} = wL^2/4$ versus $M_A^I = wL^2/8)$. The corresponding diagrams of the shear force and bending moment for the beams from Figure 4, in the case $a = b = L/2$, are shown in Figure 5.

Figure 6(a) shows the variation of deflections $v_C^I(a)$ and $v_C^{II}(a)$ for beams in Figure 4(a) and 4(b) with the position of the hinge $(0 \le a \le L)$. In the mathematical limit as $a \to L$, the hinged structure from Figure 4(b) behaves as a cantilever beam, so that $v_C^{II} \to wL^4/8EI$. It is tacitly assumed in performing the mathematical limit that the extent of the link BC approaches the infinitesimal length $wL^4/8EI$, so that the hinge C ends right below the support B. The corresponding deflection $v_C^{II}(L) = 0.125\,wL^4/EI$ is about 23 times greater than the maximum deflection in a propped cantilever from Figure 4(a), which is $v_C^I(0.5785L) \simeq 0.0054\,wL^4/EI$.

Redistribution of reactions in a fixed-end beam by a hinge

Similar analysis can be performed to determine the redistribution of reactions at A and B in the fixed-end beam from Figure 7(a), caused by the insertion of a hinge at

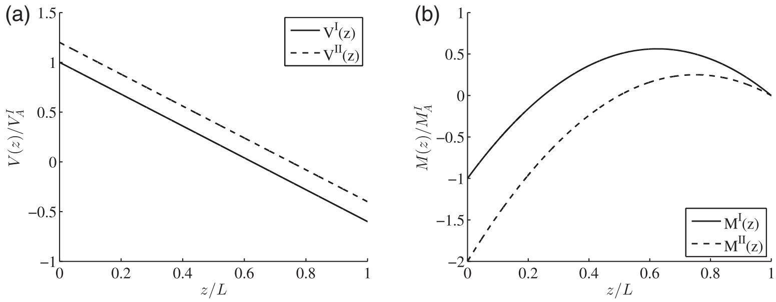

Figure 5. The plots of (a) shear force $V(z)$ (scaled by $V_A^I = 5wL/8$), and (b) bending moment $M(z)$ (scaled by $M_A^I = wL^2/8$) for the beams shown in Figure 4(a) and 4(b), when $a = 0.5\ L$. The usual conventions for positive bending moment and shear force were used in making the plots.

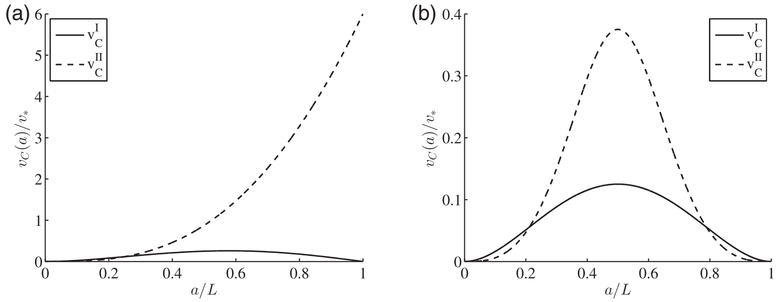

Figure 6. The deflection of the point C (scaled by $v_* = wL^4/48EI$) versus its position a/L for the beam structures in (a) Figure 4(a) and 4(b), and (b) Figure 7(a) and 7(b).

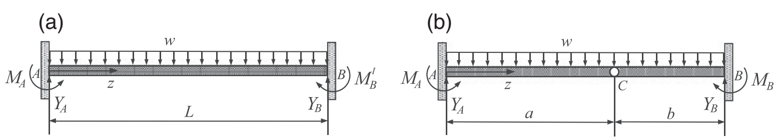

Figure 7. (a) A fixed-end beam of length L under uniformly distributed load w (case I). (b) A fixed-end beam from part (a) with an inserted hinge at point C (case II).

$z = a$ (Figure 7(b)). The well-known results (Beer et al., 2014) for a fixed-end beam of length L are

$$Y_A^I = Y_B^I = \frac{1}{2}\,wL, \quad M_A^I = M_B^I = \frac{1}{12}\,wL^2, \quad v^I(z) = \frac{wL^4}{24EI}\left(\frac{z}{L}\right)^2\left(\frac{z}{L} - 1\right)^2 \tag{29}$$

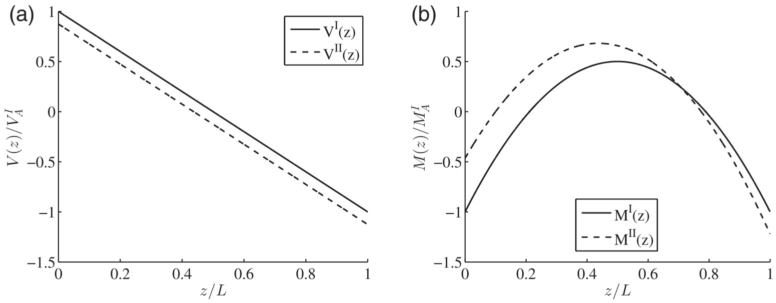

Figure 8. The plots of (a) shear force $V(z)$ (scaled by $V_A^I = wL/2$), and (b) bending moment $M(z)$ (scaled by $M_A^I = wL^2/12$) for the beams shown in Figure 7(a) and (b), when $a = L/10$.

In view of (20), it readily follows that

$$\frac{Y_A^{II}}{Y_A^I} = \frac{a}{4(a+b)}\left(5 + \frac{3b^3/a}{a^2+b^2-ab}\right), \quad \frac{M_A^{II}}{M_A^I} = \frac{3a^2}{2(a+b)^2}\left(1 + \frac{3b^3/a}{a^2+b^2-ab}\right)$$

The results for $a = b$ could have been recognized immediately. If the hinge is inserted in the middle of a fixed-end beam, it cannot transmit any force (by symmetry), and each half of a hinge-connected structure is in the state of a cantilever beam. Thus $Y_A^{II} = wa$ and $M_A^{II} = wa^2/2$. Since, $Y_A^I = wa$ and $M_A^I = wa^2/3$ (because $L = 2a$), we have $Y_A^{II}/Y_A^I = 1$ and $M_A^{II}/M_A^I = 3/2$. Therefore, the introduction of a hinge in the middle of a fixed-end beam increases the reactive moment at its ends by 50%. The diagrams of the shear force and bending moment for the beams from Figure 7(a) and 7(b) in the case $a = 0.1L$ are shown in Figure 8(a) and (b).

Figure 6(b) shows the variation of deflections $v_C^I(a)$ and $v_C^{II}(a)$ with the position of the hinge $(0 \leq a \leq L)$. If the hinge is in the middle of the structure, $v^{II}(0.5L) = wL^4/128EI$. Since the mid-deflection of the fixed-end beam from Figure 7(a) is $v_C^I(0.5L) = wL^4/384EI$, the introduction of the hinge increases the maximum deflection three times.

Various other aspects of the force and displacement redistribution caused by the insertion of a hinge can be pursued, which may be of interest for structural analysis and engineering design. For example, one may control the location of a hinge to achieve a desired value of stress or displacement at a specified location of the structure. The effect of the hinge on the magnitude of the maximum load that can be transmitted by the beam is pursued next.

Allowable stress design

The objective is now to compare the maximum load that can be carried by the considered beam structures with and without inserted hinge (Figure 4 and 7), respecting the classical design criterion according to which the maximum magnitude of the bending stress must not be greater than the yield stress σ_Y, i.e.

$$\frac{|M|_{\max}}{S} \leq \sigma_Y, \quad S = \frac{I}{|y|_{\max}} \tag{30}$$

The section modulus is denoted by S, and $|y|_{\max}$ is the maximum y-distance of the point within the cross section from the neutral (x) axis, passing through the centroid of the cross section. We consider first a propped cantilever and then a fixed-end beam. The limit design analysis based on the consideration of the plastic collapse mechanisms will be presented in the subsequent section.

Propped cantilever

The maximum magnitude of the bending moment in a propped cantilever from Figure 4(a) is $|M|_{\max} = wL^2/8$, which is the magnitude of the reactive moment (M_A) at the fixed end A. Thus, from equation (30), the maximum load before the onset of plastic yield is

$$w_{\max}^Y = \frac{8S\sigma_Y}{L^2} \tag{31}$$

For a hinged structure in Figure 4(b), the reactions at A, and the extreme value of the moment $M_m = M(z_m)$, where $z_m = Y_A/w$ specifies the cross section of the vanishing shear force, are

$$Y_A = \frac{wL}{2}\left(1 + \frac{a}{L}\right), \quad M_A = \frac{wL^2}{2}\frac{a}{L}, \quad M_m = \frac{Y_A^2}{2w} - M_A \tag{32}$$

The variations of M_A and M_m with the position of hinge a/L are shown in Figure 9(a). The maximum magnitude of the bending moment is either M_A or M_m, depending on a/L, such that

$$|M|_{\max} = \begin{cases} M_m, & \dfrac{a}{L} \leq 3 - 2\sqrt{2} \\ M_A, & \dfrac{a}{L} \geq 3 - 2\sqrt{2} \end{cases} \tag{33}$$

i.e.

$$|M|_{\max} = \frac{wL^2}{8}\begin{cases} (1 - a/L)^2, & \dfrac{a}{L} \leq 3 - 2\sqrt{2} \\ 4(a/L), & \dfrac{a}{L} \geq 3 - 2\sqrt{2} \end{cases} \tag{34}$$

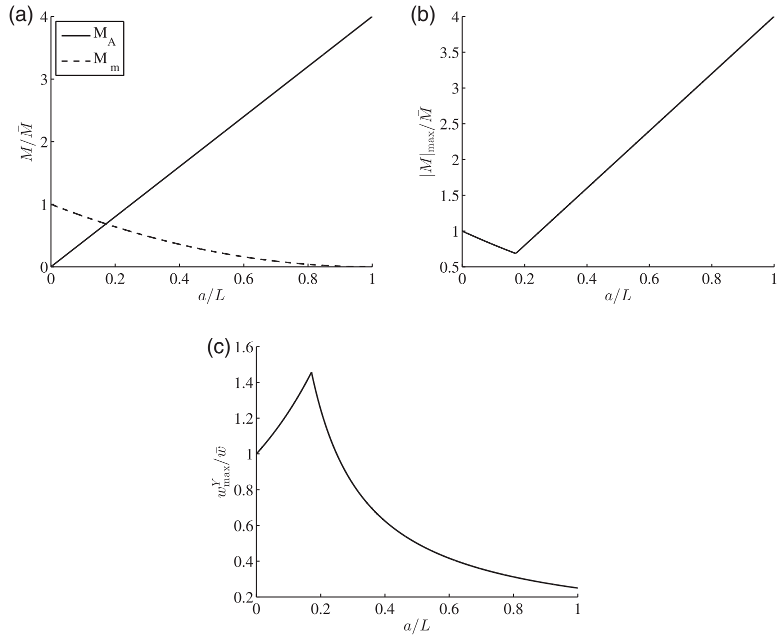

Figure 9. (a) The variations of M_A and M_m with the position of the hinge a/L in the structure shown in Figure 4(b). The scaling factor is $\bar{M} = wL^2/8$. (b) The corresponding variation of the maximum magnitude of the bending moment. (c) The variation of the maximum allowable load $w^Y_{\max}$, scaled by $\bar{w} = 8S\sigma_Y/L^2$.

This is plotted in Figure 9(b). Consequently, from equation (30), the maximum allowable load is

$$w^Y_{\max} = \frac{8S\sigma_Y}{L^2} \begin{cases} \dfrac{1}{(1-a/L)^2}, & \dfrac{a}{L} \le 3 - 2\sqrt{2} \\ \dfrac{1}{4a/L}, & \dfrac{a}{L} \ge 3 - 2\sqrt{2} \end{cases} \tag{35}$$

The variation of $w^Y_{\max}$ with a/L is shown in Figure 9(d). If a hinge is placed at $a < 0.25\ L$, the hinged structure in Figure 4(b) can transmit a greater maximum load than a propped cantilever from Figure 4(a). At first sight, this hinge-induced increase of the loading capacity is a surprising outcome of the analysis, but it may by easily explained by observing that, for $a < L/4$, the reactive moment $M_A = waL/2$ of a hinged structure from Figure 4(b) becomes smaller than the reactive moment $M_A = wL^2/8$ of a propped cantilever from Figure 4(a). The maximum load ($w^Y_{\max} = 1.4569\,\bar{w}$) is transmitted when the hinge is placed at $a = (3 - 2\sqrt{2})L \simeq 0.1716\,L$, and is 1.4569 times greater than the maximum load transmitted by a propped cantilever ($\bar{w}$). Figure 10 shows the plots of the deflection $v(z)$ in a propped cantilever from Figure 4(a) and the hinged structure from Figure 4(b) in the case

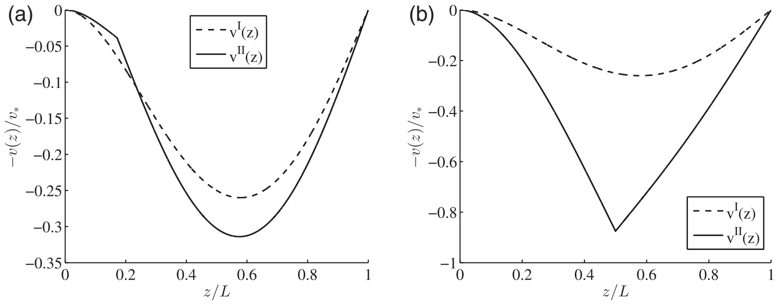

Figure 10. The deflected shape of a propped cantilever from Figure 4(a), $v^I(z)$, and the hinged structure from Figure 4(b), $v^{II}(z)$, in the case: (a) $a = 0.1716\ L$ and (b) $a = 0.5\ L$. The scaling factor is $v_* = wL^4/48EI$.

$a = 0.1716\ L$ and $a = 0.5\ L$. The overall increase of the deflection produced by the inserted hinge is naturally much greater in the latter case.

Fixed-end beam

The maximum magnitude of the bending moment in a fixed-end beam in Figure 7(a) is $|M|_{\max} = wL^2/12$, which is the magnitude of the reactive moment at the ends A and B. Thus, from equation (30), the maximum allowable load is

$$w^Y_{\max} = \frac{12S\sigma_Y}{L^2} \tag{36}$$

For the hinged structure in Figure 7(b), the reactive moments at two fixed ends are specified by equations (19) and (20), such that

$$\begin{aligned} M_A &= \frac{wL^2}{8}\,\frac{a}{L}\left[\frac{a}{L} + 3\,\frac{(1-a/L)^3}{3(a/L)^2 - 3(a/L) + 1}\right] \\ M_B &= \frac{wL^2}{8}\left(1 - \frac{a}{L}\right)\left[1 - \frac{a}{L} + 3\,\frac{(a/L)^3}{3(a/L)^2 - 3(a/L) + 1}\right] \end{aligned} \tag{37}$$

The extreme value of the moment $M_m = M(z_m)$, where $z_m = Y_A/w$, is

$$M_m = \frac{Y_A^2}{2w} - M_A, \quad Y_A = \frac{wL}{8}\left[5\,\frac{a}{L} + 3\,\frac{(1-a/L)^3}{3(a/L)^2 - 3(a/L) + 1}\right] \tag{38}$$

The plots of M_A, M_B, and M_m with a/L are shown in Figure 11(a). The hinge is passive if $a = 0.2113\ L$ or $a = 0.7887\ L$, since then $M_A = \bar{M} = wL^2/12$ in the first

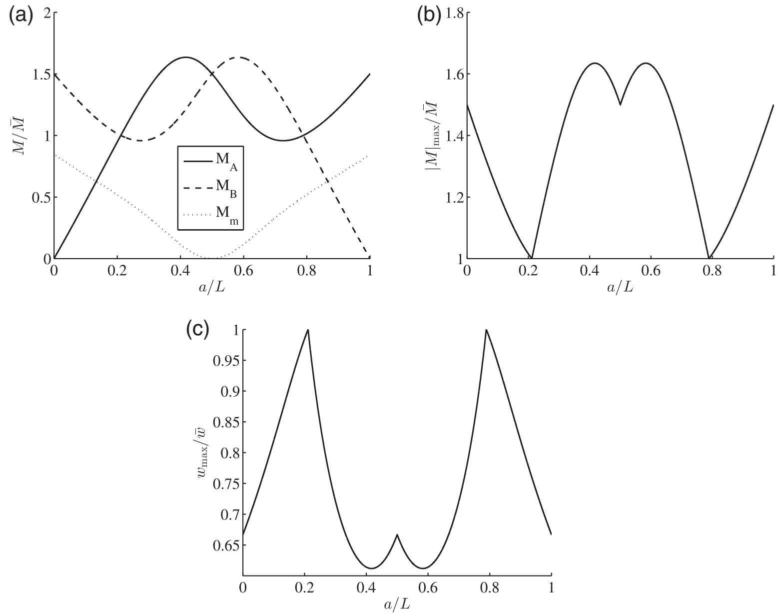

Figure 11. (a) The variations of M_A, M_B, and M_m with the position of the hinge a/L in the structure from Figure 9(b). The scaling factor is $\bar{M} = wL^2/12$. (b) The corresponding variation of the maximum magnitude of the bending moment. (c) The variation of the maximum allowable load $w^Y_{\max}$, scaled by $\bar{w} = 12S\sigma_Y/L^2$.

case, and $M_B = \bar{M} = wL^2/12$ in the second case. The maximum magnitude of the bending moment is

$$|M|_{\max} = \begin{cases} M_B, & 0 \le \dfrac{a}{L} \le 0.2113 \\ M_A, & 0.2113 < \dfrac{a}{L} \le 0.5 \\ M_B, & 0.5 \le \dfrac{a}{L} \le 0.7887 \\ M_A, & 0.7887 \le \dfrac{a}{L} \le 1 \end{cases} \tag{39}$$

which is shown in Figure 11(b). The greatest bending moment $|M|_{\max} \simeq 1.6346\,\bar{M}$ occurs when the hinge is placed at $a = 0.4171\ L$ or $a = 0.5829\ L$, and is 63.46% greater than the maximum bending moment in the fixed-end beam without a hinge. If the hinge is placed in the middle of a fixed-end beam, the maximum bending moment increases by 50%.

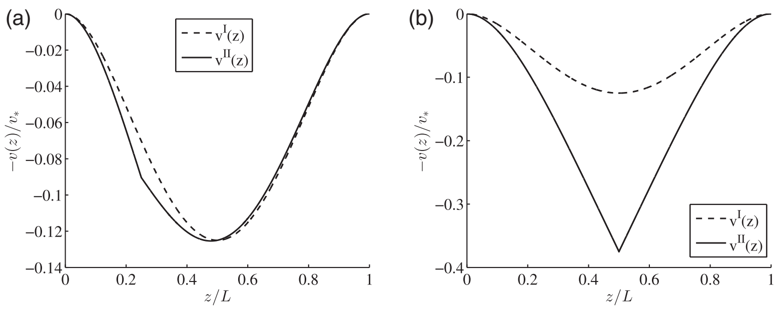

Figure 12. The deflected shape of a fixed-end beam from Figure 7(a), $v^I(z)$, and the hinged structure from Figure 7(b), $v^{II}(z)$, in the case: (a) $a = 0.25\ L$ and (b) $a = 0.5\ L$. The scaling factor is $v_* = wL^4/48EI$.

When equation (37) is substituted into equation (39), and this into equation (30), the maximum load is found to be

$$w_{\max}^Y = \frac{8S\sigma_Y}{L^2}\begin{cases} \left(1-\frac{a}{L}\right)^{-1}\left[1-\frac{a}{L}+3\,\frac{(a/L)^3}{3(a/L)^2-3(a/L)+1}\right]^{-1}, & 0 \le \frac{a}{L} \le 0.2113 \\ \left(\frac{a}{L}\right)^{-1}\left[\frac{a}{L}+3\,\frac{(1-a/L)^3}{3(a/L)^2-3(a/L)+1}\right]^{-1}, & 0.2113 \le \frac{a}{L} \le 0.5 \\ \left(1-\frac{a}{L}\right)^{-1}\left[1-\frac{a}{L}+3\,\frac{(a/L)^3}{3(a/L)^2-3(a/L)+1}\right]^{-1}, & 0.5 \le \frac{a}{L} \le 0.7887 \\ \left(\frac{a}{L}\right)^{-1}\left[\frac{a}{L}+3\,\frac{(1-a/L)^3}{3(a/L)^2-3(a/L)+1}\right]^{-1}, & 0.7887 \le \frac{a}{L} \le 1 \end{cases} \tag{40}$$

The corresponding plot is shown in Figure 11(c). The insertion of a hinge decreases the allowable load for any a/L. The decrease is greatest for $a = 0.4171\ L$, when $w_{\max}^Y = 0.6118\,\bar{w}$. For a hinge in the middle ($a = L/2$), the allowable load is $w_{\max}^Y = (2/3)\bar{w}$, where $\bar{w} = 12S\sigma_Y/L^2$. Figure 12 shows the plots of the deflection $v(z)$ in a fixed-end beam from Figure 7(a) and a hinged structure from Figure 7(b) in the case $a = 0.25\ L$ and $a = 0.5\ L$. As expected, the overall increase of the deflection produced by the inserted hinge is much greater in the latter case. The consideration of the maximum deflection places its own restriction on the maximum load, if the maximum deflection is constrained to be smaller than a prescribed value.

Limit design by collapse mechanisms

In this section, we determine the ultimate load capacity according to the limit design analysis. The ultimate load is the load at which the structure fails by

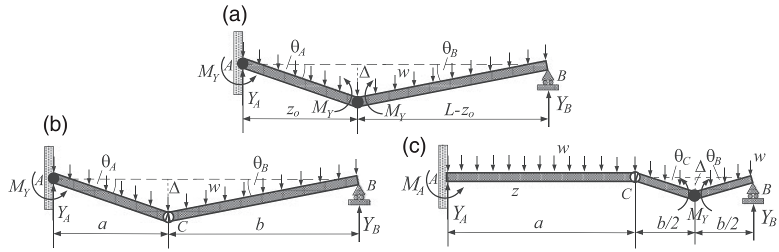

Figure 13. (a) A collapse mechanism of a propped cantilever from Figure 4(a), with plastic hinges formed at the end *A* and at a distance z_0 from it. Two plausible collapse mechanisms of the hinged structure from Figure 4(b). In the mechanism shown in part (b), the plastic hinge formed at the fixed end *A*, and in part (c) in the middle between the points *C* and *B*.

becoming a collapse mechanism, i.e. a linkage of rigid bars connected by plastic hinges (Cook and Young, 1999; Lubliner, 2008). Assuming ideal plasticity (no strain hardening), the plastic hinge allows relative rotation of adjacent bars with constant resisting (yield) moment $M_Y = \sigma_Y(A_0/2)\bar{y}_0$. The plastic neutral axis divides the cross-sectional area A_0 into two equal halves, whose centroids are at the distance $\bar{y}_0$ from each other. For example, if the cross section is rectangular, with the dimensions $B \times H$, the yield moment is $M_Y = \sigma_Y(\mathrm{BH}^2/4)$. The quantity $BH^2/4$ is the plastic section modulus of the rectangular cross section. Its elastic section modulus is $S = I/|y|_{\max} = \mathrm{BH}^2/6$. We consider first a propped cantilever and then a fixed-end beam with an inserted hinge. The ultimate load is determined from the virtual work equation, which states that "the external work of applied loads on the virtual deflection of the considered collapse mechanism" minus "the internal work of the resisting yield moments on relative rotations of adjacent bars at plastic hinges" must be equal to zero. The calculated ultimate loads will then be compared with the allowable loads determined by the classical design criterion from the previous section.

Propped cantilever

Figure 13(a) shows a collapse mechanism of a propped cantilever from Figure 4(a). Plastic hinges are assumed to form at the end A and at the distance z_0 from it. The infinitesimal virtual deflection at z_0 is denoted by Δ, and the angles of rotation at A and B by θ_A and θ_B. The corresponding virtual work equation ($\delta W = 0$) is

$$\frac{1}{2}\, wL\Delta - M_Y\theta_A - M_Y(\theta_A + \theta_B) = 0, \quad \theta_A = \frac{\Delta}{z_0}, \quad \theta_B = \frac{\Delta}{L - z_0} \tag{41}$$

which gives

$$w = \frac{2M_Y}{L}\left(\frac{2}{z_0} + \frac{1}{L - z_0}\right) \tag{42}$$

The ultimate load is obtained by minimizing equation (42) with respect to z_0 ($\mathrm{d}w/\mathrm{d}z_0 = 0$), from which

$$z_0^2 - 4Lz_0 + 2L^2 = 0 \quad \Rightarrow \quad z_0 = (2 - \sqrt{2})L \simeq 0.5858\,L \tag{43}$$

The substitution of equation (43) into equation (42) specifies the ultimate load

$$w_{\max}^{\mathrm{u}} = (3 + 2\sqrt{2})\,\frac{2M_Y}{L^2} \tag{44}$$

For the hinged structure from Figure 4(b), depending on the location of the hinge C, the collapse mechanism can be either the mechanism shown in Figure 13(b) or 13(c). For the mechanism in Figure 13(b), the virtual work equation is

$$\frac{1}{2}\,wL\Delta - M_Y\theta_A = 0, \quad \theta_A = \frac{\Delta}{a} \tag{45}$$

giving

$$w = \frac{1}{a/L}\,\frac{2M_Y}{L^2} \tag{46}$$

For the mechanism in Figure 13(c), the virtual work equation is

$$\frac{1}{2}\,wb\Delta - M_Y(\theta_B + \theta_C) = 0, \quad \theta_B = \theta_C = \frac{2\Delta}{b} \tag{47}$$

so that, in this case

$$w = \frac{4}{(1 - a/L)^2}\,\frac{2M_Y}{L^2} \tag{48}$$

For each a/L, the true ultimate load is the smaller of the two values in equations (46) and (48). Thus

$$w_{\max}^{\mathrm{u}} = \frac{2M_Y}{L^2}\begin{cases} \dfrac{4}{(1 - a/L)^2}, & \dfrac{a}{L} \leq 3 - 2\sqrt{2} \\ \dfrac{1}{a/L}, & \dfrac{a}{L} \geq 3 - 2\sqrt{2} \end{cases} \tag{49}$$

The variation of $w_{\max}^{\mathrm{u}}$ with a/L is shown in Figure 14(a). The ratio a/L separating the two intervals in equation (49) is $3 - 2\sqrt{2} \simeq 0.1716$. At this ratio the ultimate load for both mechanisms from Figure 13(b) and (c) is equal to the ultimate load of a propped cantilever from Figure 13a, which is $\bar{w} = 2(3 + 2\sqrt{2})M_Y/L^2$. For all

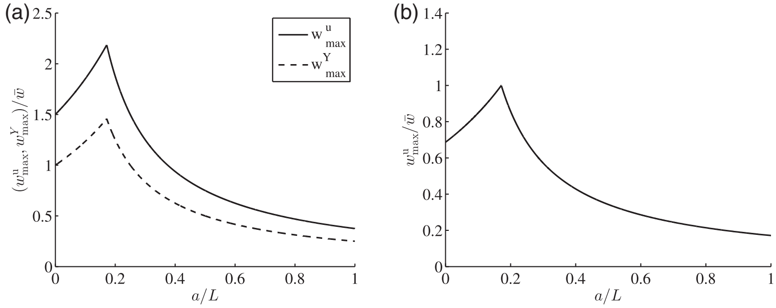

Figure 14. (a) The variation of the ultimate load $w^{\mathrm{u}}_{\mathrm{max}}$ of the hinged structure from Figure 4(a) with a/L. The scaling factor is $\bar{w} = 2(3 + 2\sqrt{2})M_Y/L^2$. (b) The plots of w^{Y}_{max} and $w^{\mathrm{u}}_{\mathrm{max}}$, both normalized by $\bar{w} = (4/3)\sigma_Y BH^2/L^2$, in the case of the rectangular cross section with the dimensions $B \times H$.

other ratios a/L, the ultimate load for the mechanisms in Figure 13(b) and (c) is lower than the ultimate load of a propped cantilever from Figure 13(a).

Figure 14(b) shows the plots of w^{Y}_{max}, as specified by equation (35), and $w^{\mathrm{u}}_{\mathrm{max}}$, as specified by (49), together. It is assumed that the cross section is rectangular with the dimensions $B \times H$, so that $S = \mathrm{BH}^2/6$ and $M_Y = \sigma_Y \mathrm{BH}^2/4$. The scaling factor for both plots is $\bar{w} = (4/3)\sigma_Y BH^2/L^2$, which is the load at the onset of first yield in a propped cantilever from Figure 4(a). In this case, the two ultimate loads are related by $w^{\mathrm{u}}_{\mathrm{max}} = (3/2)w^{Y}_{\mathrm{max}}$ for all a/L.

Fixed-end beam

Figure 15(a) shows a collapse mechanism of a fixed-end beam from Figure 7(a), with plastic hinges formed at the ends A and B, and in the middle of the beam. The corresponding virtual work equation is

$$\frac{1}{2}\,wL\Delta - M_Y\theta_A - M_Y\theta_B - M_Y(\theta_A + \theta_B) = 0, \quad \theta_A = \theta_B = \frac{2\Delta}{L} \tag{50}$$

which gives the ultimate load

$$w^{\mathrm{u}}_{\mathrm{max}} = 8\,\frac{2M_Y}{L^2} \tag{51}$$

For a hinged structure from Figure 7(b), depending on the location of the hinge C, the collapse mechanism can be either the mechanism shown in Figure 15(b) or 15(c). For the mechanism in Figure 15(b), the virtual work equation is

$$\frac{1}{2}\,wb\Delta - M_Y\theta_B - M_Y(\theta_B + \theta_C) = 0, \quad \theta_B = \frac{\Delta}{b - z_1}, \quad \theta_C = \frac{\Delta}{z_1} \tag{52}$$

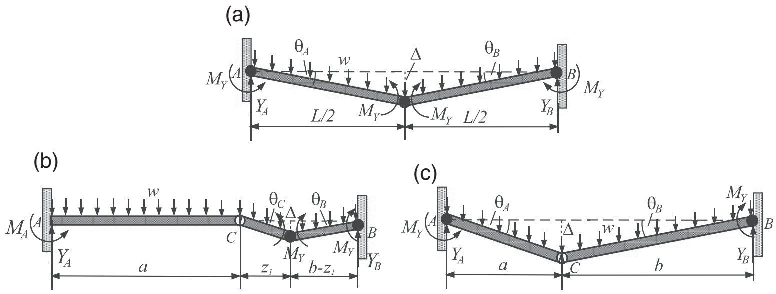

Figure 15. (a) A collapse mechanism of a fixed-end beam from Figure 9(a), with plastic hinges formed at the ends *A* and *B*, and in the middle of the span. Two plausible collapse mechanisms of the hinged structure from Figure 9(b). In the mechanism shown in part (b), the plastic hinges formed at the fixed end *B*, and at a distance z_1 from *C*. In the mechanism shown in part (c), the plastic hinges formed at the fixed ends *A* and *B*.

from which

$$w = \frac{2M_Y}{L}\left(\frac{2}{b - z_1} + \frac{1}{z_1}\right) \tag{53}$$

The ultimate load is obtained by minimizing equation (53) with respect to z_1 ($\mathrm{d}w/\mathrm{d}z_1 = 0$). This gives

$$z_1^2 + 2bz_1 - b^2 = 0 \quad \Rightarrow \quad z_1 = (\sqrt{2} - 1)b \simeq 0.4142\, b \tag{54}$$

The substitution of equation (54) into equation (53) specifies the load

$$w = (3 + 2\sqrt{2})\,\frac{2M_Y}{b^2} \tag{55}$$

For the mechanism in Figure 15(c), the virtual work equation is

$$\frac{1}{2}\,wL\Delta - M_Y\theta_A - M_Y\theta_B = 0, \quad \theta_A = \frac{\Delta}{a}, \quad \theta_B = \frac{\Delta}{b} \tag{56}$$

so that

$$w = \frac{2M_Y}{ab} \tag{57}$$

The true ultimate load, for each a/L, is the smaller of the two values in equations (55) and (57). Thus,

$$w_{\max}^{\mathrm{u}} = \frac{2M_Y}{L^2} \begin{cases} \dfrac{3+2\sqrt{2}}{(1-a/L)^2}, & \dfrac{a}{L} \leq 0.1464 \\ \dfrac{1}{(a/L)(1-a/L)}, & \dfrac{a}{L} \geq 0.1464 \end{cases} \tag{58}$$

The value of the ratio $a/L \simeq 0.1464$ was obtained by equating the two equations (55) and (57), i.e.

$$\frac{2M_Y}{ab} = 2(2+\sqrt{2})\frac{M_Y}{b^2} \quad \Rightarrow \quad (a/L)^2 - (5+2\sqrt{2})(a/L) + 1 = 0 \quad \Rightarrow \quad a/L \simeq 0.1464$$

The variation of $w_{\max}^{\mathrm{u}}$ with a/L is shown in Figure 16(a). The scaling load is $\bar{w} = 16M_Y/L^2$, which is the ultimate load of a fixed-end beam from Figure 7(a). Only half of that load would be the limiting load if the hinge C was placed in the

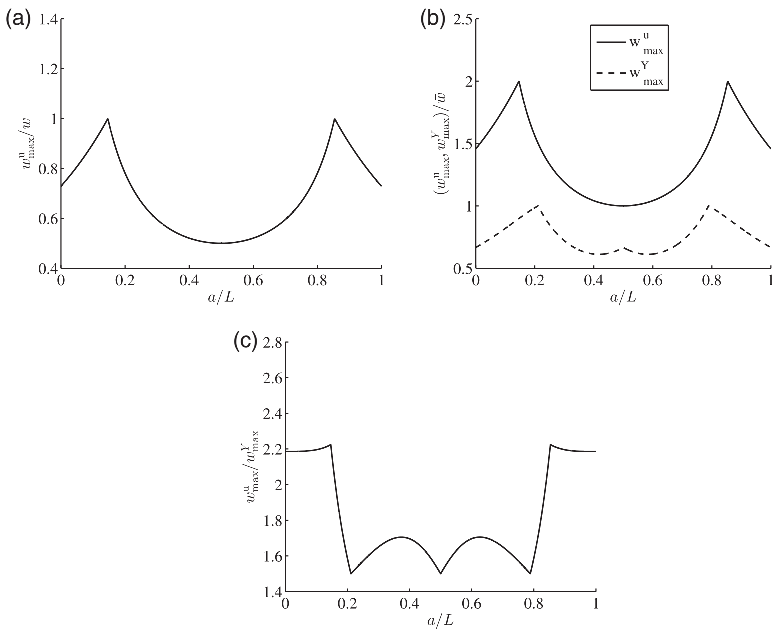

Figure 16. (a) The variation of the ultimate load $w_{\max}^{\mathrm{u}}$ of the hinged structure from Figure 7(a) with a/L. The scaling factor is $\bar{w} = 16M_Y/L^2$. (b) The plots of $w_{\max}^{Y}$ and $w_{\max}^{\mathrm{u}}$, both normalized by $\bar{w} = 2\sigma_Y BH^2/L^2$, in the case of the rectangular cross section with the dimensions $B \times H$. (c) The variation of the load ratio $w_{\max}^{\mathrm{u}}/w_{\max}^{Y}$ with a/L.

middle of a fixed-end beam. For all ratios a/L, the ultimate load of a fixed-end beam from Figure 7(a) is greater than the ultimate load of the hinged structure from Figure 7(b).

Figure 16(b) shows the plots of $w^{Y}_{\max}$, as specified by equation (40), and $w^{\mathrm{u}}_{\max}$, as specified by equation (58), together. The cross section is assumed to be rectangular with the dimensions $B \times H$. The scaling factor for both plots is $\bar{w} = 2\sigma_Y BH^2/L^2$, which is the load at the onset of first yield in the fixed-end beam from Figure 7(a). In contrast to the case of a hinge-relaxed propped cantilever (Figure 4(b)), for which the load ratio $w^{\mathrm{u}}_{\max}/w^{Y}_{\max} = 3/2$ is constant, in the case of a hinge-relaxed fixed-end beam (Figure 7(b)), the ratio $w^{\mathrm{u}}_{\max}/w^{Y}_{\max}$ varies with a/L. The variation is shown in Figure 16(c). The maximum load ratio is about 2.2246, at $a/L = 0.1464$ and $a/L \simeq 0.8536$. The minimum load ratio is equal to 1.5, at $a/L \simeq 0.2113$ and $a/L \simeq 0.7887$.

Conclusions

The internal forces and deflections are determined for the structure consisting of two hinge-connected beams, whose left end is fixed and right end simply supported. The loading consists of a uniformly distributed load along the entire length of the structure, and a concentrated couple at the right end. The solution is obtained by an extended use of the method of discontinuity functions to incorporate the slope discontinuity at the hinge, without the separation of the structure into two parts, commonly done in other methods of analysis. Based on the derived general formulas, the redistribution of internal forces and deflections, caused by the insertion of a frictionless hinge, is evaluated in a propped cantilever and a fixed-end beam. It is shown that a hinge placed in the middle of a propped cantilever increases the reactive moment at the fixed end two times, while its insertion in the middle of a fixed-end beam increases its reactive moments by 50%. The mid-deflection of a fixed-end beam increases three times by the introduction of a hinge.

The maximum allowable load is then determined by using the classical and the limit design criteria. According to the classical design criterion, if the hinge is placed in a propped cantilever at the distance from its fixed end less than one-fourth of its span ($a < L/4$), the hinged structure can transmit a greater distributed load than a propped cantilever without a hinge. The maximum load that a hinged structure can transmit is about 46% greater than the maximum load transmitted by a propped cantilever without a hinge. However, according to the limit design criterion, the insertion of a hinge in a propped cantilever decreases the limit load for any a/L. On the other hand, the insertion of a hinge in a fixed-end beam decreases the maximum load according to both design criteria, for any position of the hinge. The classical design criterion in this case predicts the greatest load decrease if a hinge is placed at $a = 0.4171\ L$, the maximum load is about 61% of the maximum load transmitted by a fixed-end beam without a hinge. According to the limit design criterion, the load decrease is greatest for $a = 0.5\ L$, when it is 50% of the maximum load transmitted by a fixed-end beam without a hinge. For rectangular cross-sections, the ratio of the maximum load according to the limit and the classical design criterion is constant and equal to 3/2 in the case of a hinge-relaxed propped cantilever, while it varies with a/L in the case of a hinge-relaxed fixed-end beam. In the latter case, the greatest load ratio is about 2.225, while the lowest value of this ratio is equal to 1.5.

Apart from its practical importance for the analysis of various structural systems in mechanical and civil engineering, the presented evaluation of the deflection and force redistribution caused by insertion of a frictionless hinge, and the corresponding calculation of allowable and ultimate loads based on classical and limit design criteria, is important for engineering education and the development of student ability to design and analyze structural systems, which is one of the ABET student outcomes criterion for accrediting engineering programs (ABET, 2015).

Declaration of Conflicting Interests

The author(s) declared no potential conflicts of interest with respect to the research, authorship, and/or publication of this article.

Funding

The author(s) received no financial support for the research, authorship, and/or publication of this article.

References

1. ABET. *Accreditation criterion and supporting documents*. 2015; Available at: http://www.abet.org/eac-criteria-2014-2015.
2. Attaway S. *Matlab - A Practical Introduction to Programming and Problem Solving*, 3rd ed. Amsterdam: Butterworth-Heinemann, 2013.
3. Beer FP, Johnston ER Jr, DeWolf JT and Mazurek DF. *Mechanics of Materials*, 7th ed. New York: McGraw-Hill, 2014.
4. Brungraber RJ. Singularity functions in the solution of beam-deflection problems. *International Journal of Engineering Education* 1965; 155(9): 278–280.
5. Budynas R and Nisbett K. *Shigley's Mechanical Engineering Design*. New York: McGraw-Hill, 2014.
6. Cook RD and Young WC. *Advanced Mechanics of Materials*, 2nd ed. New Jersey: Prentice Hall, 1999.
7. Craig RR Jr. *Mechanics of Materials*, 3rd ed. New York: John-Wiley & Sons, 2011.
8. Failla G. Closed-form solutions for Euler–Bernoulli arbitrary discontinuous beams. *Archive of Applied Mechanics* 2011; 81(5): 605–628.
9. Falsone G. The use of generalised functions in the discontinuous beam bending differential equations. *International Journal of Engineering Education* 2002; 18(3): 337–343.
10. Gere JM and Goodno BJ. *Mechanics of Materials*, 8th ed. Toronto: Cengage Learning, 2013.
11. Lubliner J. *Plasticity Theory*. Mineola, New York: Dover Books on Engineering, 2008.
12. Yavari A, Sarkani S and Moyer ET. On applications of generalized functions to beam bending problems. *International Journal of Solids and Structures* 2000; 37(40): 5675–5705.